

Habitual foot strike pattern does not affect simulated Triceps Surae muscle metabolic energy consumption during running

Wannes Swinnen¹, Wouter Hoogkamer², Friedl De Groot¹, Benedicte Vanwanseele¹

¹Human Movement Biomechanics Research Group, Department of Movement Sciences, KU Leuven, Leuven, Belgium

²Department of Kinesiology, University of Massachusetts Amherst, Amherst, USA

Abstract

Foot strike pattern affects ankle joint work and Triceps Surae muscle-tendon dynamics during running. Whether these changes in muscle-tendon dynamics also affect Triceps Surae muscle energy consumption is still unknown. In addition, as the Triceps Surae muscle accounts for a substantial amount of the whole body metabolic energy consumption, changes in Triceps Surae energy consumption may affect whole body metabolic energy consumption. However, direct measurements of muscle metabolic energy consumption during dynamic movements is hard. Model-based approaches can be used to estimate individual muscle and whole body metabolic energy consumption based on Hill type muscle models. In this study, we use an integrated experimental and dynamic optimization approach to compute muscle states (muscle forces, lengths, velocities, excitations and activations) of 10 habitual mid-/forefoot striking and 9 habitual rearfoot striking runners while running at 10 and 14 km/h. The Achilles tendon stiffness of the musculoskeletal model was adapted to fit experimental ultrasound data of the Gastrocnemius medialis muscle during ground contact. Next, we calculated Triceps Surae muscle and whole body metabolic energy consumption using four different metabolic energy models provided in literature. Neither Triceps Surae metabolic energy consumption ($p > 0.35$), nor whole body metabolic energy consumption ($p > 0.14$) was different between foot strike patterns, regardless of the energy model used or running speed tested. Our results provide new evidence that mid-/forefoot and rearfoot strike pattern are metabolically equivalent.

Introduction

The metabolic energy consumed during submaximal running, often referred to as running economy, is an important factor determining endurance running performance (Jones and Carter, 2000). Reduced energy consumption corresponds to improved running economy and hence superior endurance performance (Hoogkamer et al., 2016; Kipp et al., 2019). As such, runners seek to adopt a running pattern with minimal metabolic energy consumption. One aspect of people's running pattern is foot strike pattern. Although foot strike pattern is a continuum, generally three different foot strike patterns are considered: forefoot strike, midfoot strike and rearfoot strike (Cavanagh and LaFortune, 1980).

34 While rearfoot striking is the most common running pattern during shod running (Hasegawa et al.,
35 2007; Kasmer et al., 2013; Larson et al., 2011), there seems to be a widespread popular believe that
36 forefoot striking would be more economical than rearfoot striking. Previous research has
37 demonstrated that there is a greater percentage mid-/forefoot strikers among the first finishers in long
38 distance races (de Almeida et al., 2015; Hasegawa et al., 2007), which suggests that forefoot striking
39 may be more economical. However, studies comparing metabolic energy consumption between
40 habitual forefoot and habitual rearfoot strikers found no difference in whole body metabolic energy
41 consumption (Gruber et al., 2013) or even lower energy consumption in rearfoot strikers compared to
42 their forefoot striking colleagues at 11 and 13 km/h but not at 15 km/h (Ogueta-Alday et al., 2014).

43 Available analyses of the kinetic and kinematic differences between foot strike patterns do not clearly
44 provide evidence for either differences in or unchanged energy consumption with foot strike patterns.
45 The shorter ground contact times (Di Michele and Merni, 2014; Mercer and Horsch, 2015), associated
46 with forefoot striking, may increase metabolic energy consumption according to Kram and Taylor's
47 cost of generating force hypothesis (Kram and Taylor, 1990). They established that the metabolic
48 energy consumption is inversely proportional to ground contact time, which implies that forefoot
49 strikers may consume more metabolic energy. In addition, forefoot strikers demonstrate greater
50 negative ankle work compared to rearfoot strikers (Stearne et al., 2014). This ankle work is
51 predominantly absorbed by the muscle-tendon unit (MTU) spanning the ankle joint, i.e., Triceps Surae
52 muscle and the in series connected tendinous tissue (SEE, series elastic element). Hence, differences
53 in ankle work may affect the MTU and subsequently the energy consumption of this Triceps Surae
54 muscle. We recently demonstrated that in habitual mid-/forefoot strikers the Gastrocnemius medialis
55 (GM) produces greater muscle force but at lower contraction velocities during early stance compared
56 to habitual rearfoot strikers (Swinnen et al., 2019). Higher muscle force production suggests more
57 muscle activation and thus higher metabolic energy consumption, whereas lower contraction
58 velocities are more force efficient and would therefore reduce muscle activation and thus metabolic
59 energy consumption. Hence, we hypothesized that the differences in metabolic energy consumption
60 would counteract each other and no difference in GM metabolic energy consumption would exist
61 (Swinnen et al., 2019). Yet, as Fletcher and MacIntosh (2017) estimated that 25 to 40% of the total
62 whole body metabolic energy is consumed by the Triceps Surae muscle, we would expect different
63 whole body metabolic energy consumption if Triceps Surae metabolic energy consumption would be
64 different between foot strike patterns.

65 Model-based approaches have been used to estimate individual muscle and whole body metabolic
66 energy consumption based on Hill type muscle models (Bhargava et al., 2004; Miller, 2014; Uchida et
67 al., 2016; Umberger, 2010; Umberger et al., 2003). However, to obtain reliable simulation results, a

68 close match between simulated and experimental data is essential. Here, we used experimental
69 dynamics ultrasound data from the Gastrocnemius medialis (GM) to improve our dynamic
70 optimization and as such, ensure more reliable estimations of muscle metabolic energy consumption.
71 We used four different metabolic energy models (Bhargava et al., 2004; Uchida et al., 2016; Umberger,
72 2010; Umberger et al., 2003) to calculate Triceps Surae muscle and whole body metabolic energy
73 consumption of habitual mid-/forefoot and rearfoot strikers running at 10 and 14 km/h. We
74 hypothesized that neither Triceps Surae nor whole body metabolic energy consumption would be
75 different between foot strike patterns.

76 **Methods**

77 **Participants.** Ten habitual mid-/forefoot strikers (6 males, 4 females; body mass: 65.2 ± 7.7 kg;
78 body height: 1.78 ± 0.07 m) and 9 habitual rearfoot strikers (6 males, 3 females; body mass: 72.7 ± 12.5
79 kg; body height: 1.81 ± 0.08 m) participated in this study. All participants were regular runners who
80 ran at least 30 km/week, did not have any Achilles tendon or calf injury in the last six months and had
81 no prior Achilles tendon surgery. Written informed consent, approved by the local ethical committee
82 (Medical Ethical Committee of UZ Leuven), was obtained at the start of the experiment.

83 **Experimental procedure.** The experimental procedures have been described in detail in our
84 earlier publication on gastrocnemius medialis muscle-tendon interaction and muscle force production
85 in this group of runners (Swinnen et al., 2019). Briefly, after a 10 minutes warm-up, participants ran 5
86 minutes on a force measuring treadmill (Motekforce Link, Amsterdam, The Netherlands): 2.5 minutes
87 at 10 and at 14 km/h, in randomized order. We collected kinetic, kinematic, muscle activation and
88 ultrasound data of at least four strides during the last minute of each running speed. All measurements
89 were synchronized through a trigger pulse signal sent from the ultrasound device.

90 **Kinetics, kinematic and foot strike angle.** Thirteen infrared cameras (Vicon, Oxford Metrics,
91 UK) captured the motion of forty-seven reflective markers at a sampling frequency of 150 Hz. We used
92 OpenSim 3.3 (OpenSim, Stanford, USA) to first scale a musculoskeletal model based on the subject's
93 dimensions (Hamner et al., 2010) and to subsequently compute joint kinematics using a Kalman
94 smoothing algorithm (De Groot et al., 2008). Muscle tendon unit lengths were calculated using
95 OpenSim's Muscle Analysis Tool.

96 Ground reaction force data, sampled at 900 Hz, was first low pass filtered with a cut-off frequency of
97 20 Hz and used to determine ground contact phase adopting a 30 N threshold. We determined foot
98 strike angle using a marker based method (Altman and Davis, 2012). At initial ground contact, we drew
99 a line through the first metatarsal-phalangeal joint marker and heel marker of the left foot. The angle
100 between this line and the ground was calculated and considered as the foot strike angle. Following

101 Altman and Davis (2012) runners with a foot strike angle greater than 8° were considered rearfoot
102 strikers, while runners with a foot strike angle under 8° were considered mid-/forefoot strikers. Foot
103 strike angle was averaged over the strides used for ultrasound analysis. Foot strike type (rearfoot or
104 mid-/forefoot) was consistent within subjects across running speeds.

105 We calculated joint torques using OpenSim's Inverse Dynamics Tool based on joint kinematics and
106 ground reaction forces. Joint torques were low pass filtered using a recursive fourth order Butterworth
107 filter with cut-off frequency of 20 Hz.

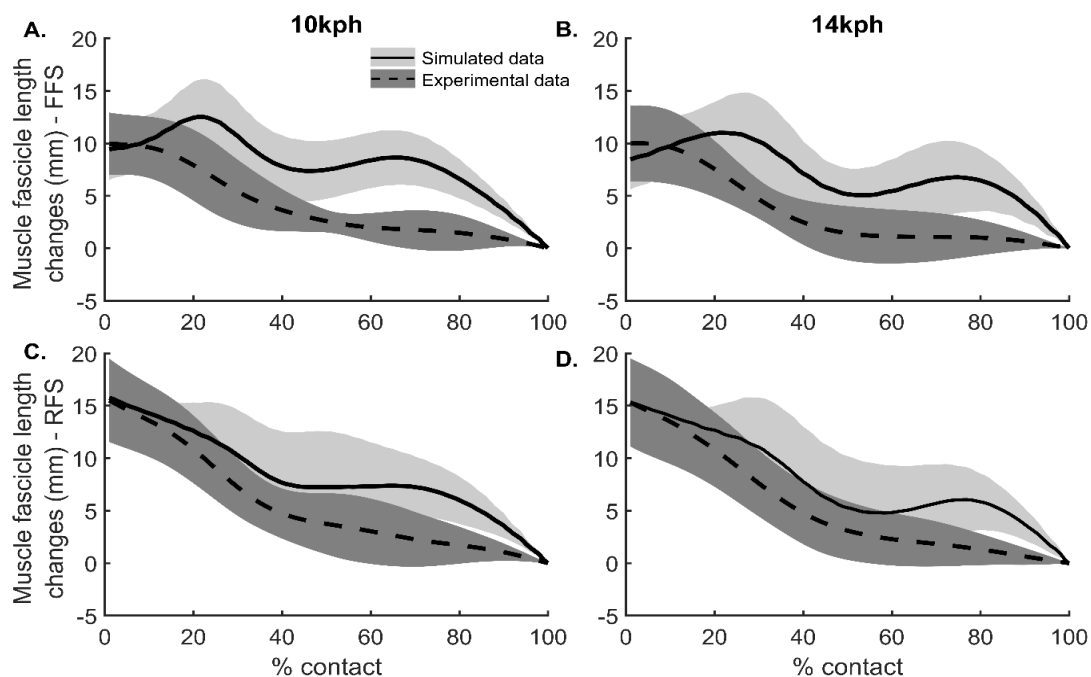
108 **Dynamic ultrasound imaging.** We collected dynamic ultrasound images of the GM muscle
109 fascicles of the left leg with a B-mode ultrasound system (Telemed Echoblaster 128 CEXT system)
110 sampling at 86 Hz. The linear transducer (UAB Telemed, Vilnius, Lithuania, LV 7.5/60/128Z-2) was
111 placed on the mid-belly of the muscle, aligned with the muscle fascicles and attached to the calf with
112 tape and bandages. To analyze the GM muscle fascicle lengths and pennation angles we used a semi-
113 automatic tracking algorithm (Farris and Lichtwark, 2016). We analyzed at least four strides and
114 calculated fascicle length changes relative to fascicle length at toe-off. All data were splined to 100
115 data points per ground contact, starting at initial contact.

116 **Muscle activity.** We used surface electromyography (EMG) to determine GM and Soleus (SOL)
117 muscle activity of the right leg through a wireless EMG acquisition system (ZeroWire EMG Aurion,
118 Milano, Italy) measuring at 900 Hz. EMG signals were first band-pass filtered (20-400 Hz), rectified and
119 low-pass filtered (20 Hz). For each subject and muscle, EMG waveforms were normalized to maximal
120 activation, determined as the maximal activation of each muscle using a moving average over 10 data
121 points. Due to technical issues, the EMG data of the GM of one participant (mid-/forefoot striker) and
122 SOL of three participants (2 mid-/forefoot strikers and 1 rearfoot striker) could not be used.

123 Comparison between experimental EMG and simulated activation of the GM and SOL demonstrated
124 similar trends, yet due to our optimization criteria (minimization of muscle activation squared) pre-
125 activation is not predicted (Fig. S1).

126 **Estimating muscle and whole body metabolic energy consumption.** Several models for
127 estimating muscle metabolic energy rate have been proposed and it is yet unclear which model yields
128 the most valid results. We, therefore, used multiple models primarily to assure that our results are
129 independent from the metabolic energy model used. Our goal was not to compare the different energy
130 models (for comparison between metabolic energy models see Miller 2014). All models required the
131 muscle states (i.e., muscle activations, excitations, lengths, velocities and forces) as inputs. To obtain
132 these muscle states we solved the muscle redundancy problem using a dynamic optimization
133 algorithm that takes into account muscle-tendon dynamics (i.e., muscle activation and contraction

134 dynamics) of the 43 lower limb muscles of the left leg in our model (De Groot et al., 2009; De Groot
135 et al., 2016). Individual muscle moment arms, muscle tendon unit lengths and muscle properties were
136 extracted from the scaled OpenSim model and were input to the muscle redundancy solver. We scaled
137 maximal isometric muscle force based on the subject's body mass and height (Handsfield et al., 2014).
138 To avoid maximal muscle activations and unrealistically high reserve actuator forces, muscle forces
139 were multiplied by 3 for all participants. The Triceps Surae muscles, containing the GM, Gastrocnemius
140 lateralis (GL) and SOL, were modeled as three separate muscle-tendon units, with the tendon
141 representing the Achilles tendon. To ensure a close match between experimental GM muscle fascicle
142 length changes and simulated GM muscle fascicle lengths, we adjusted the normalized tendon
143 stiffness, a scaling factor to calculate GM, GL, SOL tendon stiffness based on the ratio between maximal
144 isometric force and tendon slack length, to a value of 5 for all participants (Figure 1). Gerus et al. (2015)
145 previously stated that the Achilles tendon is more compliant than the generic tendon stiffness as
146 described by Zajac (1989). We tested multiple other values (ranging from 4 to 35) where 5 gave the
147 best match. The normalized stiffness for all other muscles was kept on the default value of 35. Joint
148 torques served as inputs to solve the muscle redundancy problem by minimizing the squared muscle
149 activation. We solved the dynamic optimization problem through direct collocation using GPOP-II
150 software (Patterson and Rao, 2014). Subsequently the resulting nonlinear equations was solved using
151 ipopt (Wächter and Biegler, 2006). In 9 out of the 154 ground contact analyzed the optimization
152 algorithm failed to find an optimal solution, these strides were excluded.



153

154 **Figure 1. Simulated (solid) and experimental (dashed) GM muscle fascicle length changes during ground contact in mid-
155 /forefoot strikers (A,B; n = 10) and rearfoot strikers (C,D; n = 9) at 10 km/h (A,C) and 14 km/h (B,D). Muscle fascicle length
156 changes are normalized to muscle fascicle length at toe off. Shaded area represent standard deviation.**

157 Next, the simulated muscle states were used as input in four models to estimate muscle metabolic
158 energy rate E that are consistent with Hill based muscle dynamics: Umberger, Gerritsen and Martin
159 (2003) (U2003), Bhargava, Pandya and Anderson (2004) (B2004), Umberger (2010) (U2010) and Uchida
160 *et al.* (2016) (U2016). All these models had the same general form to calculate energy expenditure:

$$161 \quad E = H_A + H_M + H_{SL} + cW$$

162 Where H_A , H_M and H_{SL} are the heat production rates of the muscles for activation, maintenance and
163 shortening/lengthening respectively, W is the muscle mechanical work rate where concentric work is
164 defined positively and C is weighting factor depending on the type of work (concentric or eccentric).
165 Major differences between the models are how they treat eccentric muscle work and how they weight
166 muscle lengthening heat rate. While in U03 and U16 negative mechanical work (i.e., metabolic energy
167 generation) is incorporated, B04 and U10 are restricted to positive mechanical work only, negative
168 mechanical work is excluded and the lengthening heat rate coefficient is adapted. Apart from these
169 differences, the heat rate calculations have similar terms between the models, though the scaling
170 factors used are different. Activation and maintenance heat rates are generally defined by muscle
171 mass/force, length and fiber type composition while shortening/lengthening heat rate depend on
172 muscle contraction velocity. U03, U10 and U16 scale these heat rates by muscle activation whereas
173 B04 does not. We refer to the specific papers for more detailed information on the models.

174 Muscle metabolic energy rate was integrated over time to obtain metabolic energy consumption
175 during one stance phase which was then multiplied by 2, to account for both legs, and multiplied by
176 the stride frequency to obtain metabolic energy rate in Watts. The metabolic energy consumed by the
177 Triceps Surae muscles was normalized to their respective muscle mass. We computed whole body
178 metabolic energy expenditure as the sum of metabolic energy consumed by all 43 muscles included in
179 the model and added a basal rate of 1.2 W/kg (Waters and Mulroy, 1999). Whole body metabolic
180 energy consumption was normalized to body mass.

181

182 **Statistics.** All data are presented as mean \pm standard deviation. We categorized our data in
183 four groups: mid-/forefoot strike at 10 km/h (FF 10), mid-/forefoot strike at 14 km/h (FF 14), rearfoot
184 strike at 10 km/h (RF 10) and rearfoot strike at 14 km/h (RF 14). First, normality was checked with the
185 Shapiro-Wilk test. If data from all groups followed a normal distribution a mixed analysis of variance
186 (ANOVA) was used to determine interaction and main effects (foot strike pattern and running speed)
187 using SPSS v.24 (IBM SPSS, Armonk, New York, USA). Yet, if not all the data in the groups followed a

188 normal distribution, the non-parametric Mann-Whitney U test was performed to compare foot strike
189 pattern differences at 10 and 14 km/h separately. To determine the effect of running speed for these
190 datasets, the data was first grouped according to running speed and again checked upon normality. If
191 both datasets were then normally distributed, a paired t-test was performed, if not we performed a
192 Wilcoxon signed-rank test. Statistical significance was considered when $p < 0.05$.

193

194 **Results**

195 Although mean foot strike angle was more than 15° different between both foot strike groups ($p <$
196 0.01 ; Table 1), Triceps Surae metabolic energy consumption was not different between foot strike
197 patterns, regardless of speed or metabolic energy model ($p > 0.35$; Figure 2). Moreover, metabolic
198 energy consumed by the individual Triceps Surae muscles, i.e. GM, GL and SOL, was not different
199 between foot strike patterns ($p > 0.10$) independent of the model used or running speed. Furthermore,
200 estimated whole body metabolic energy consumption was not different between foot strike patterns
201 regardless of model or running speed tested ($p > 0.14$; Figure 3). As one would expect, running faster
202 resulted in greater metabolic energy consumption in the Triceps Surae muscle group ($p < 0.01$) as well
203 as in all three Triceps Surae individually ($p < 0.02$). Also, whole body metabolic energy consumption
204 was greater when running at 14 km/h compared to 10 km/h ($p < 0.01$).

205 The ratio of metabolic energy consumed by the Triceps Surae relative to whole body metabolic energy
206 consumption ranged between 22 and 32% across foot strike patterns and running speeds but was not
207 different between foot strike patterns ($p > 0.19$). In contrast, the different models revealed
208 inconsistent results when the effect of speed on this ratio was considered. While U03 and U16 did not
209 show significant differences in this ratio between running speeds ($p > 0.07$), U10 showed a significant
210 greater ratio at 14km/h compared to 10 km/h ($p = 0.01$), whereas B04 showed a significant smaller
211 ratio at 14 km/h than at 10 km/h ($p = 0.02$).

212

213

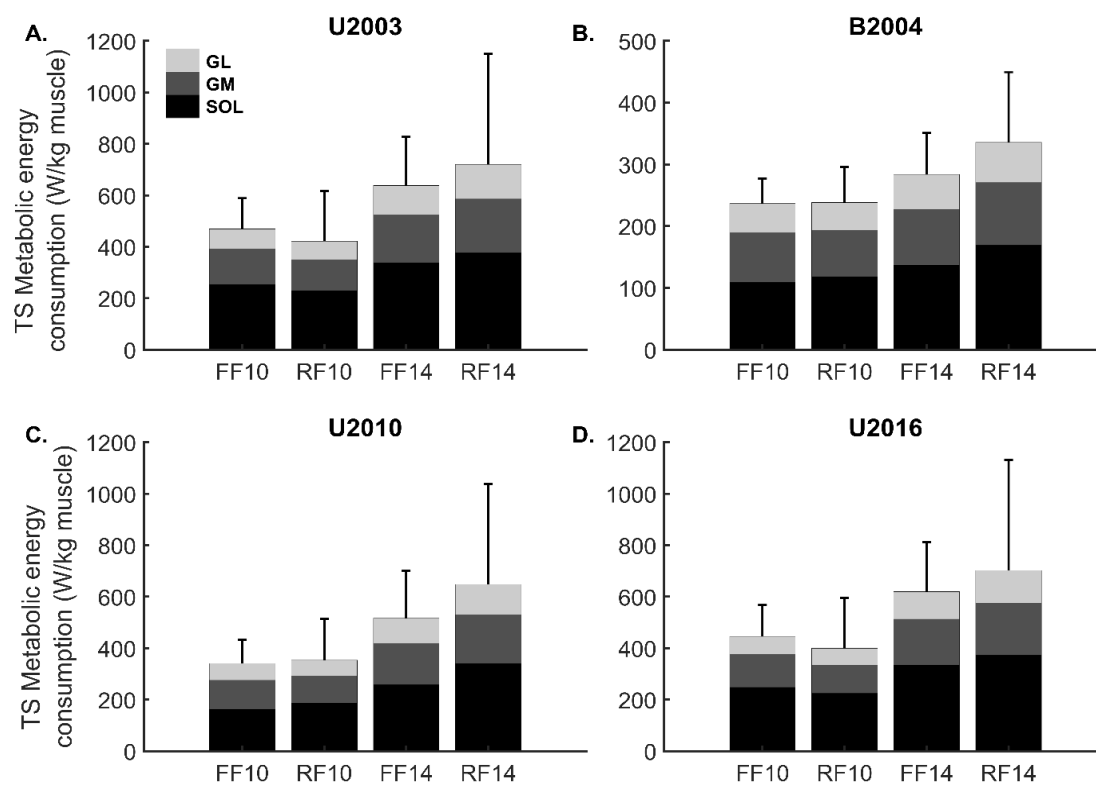
214

215

216 *Table 1 Comparison between mid-/forefoot and rearfoot strikers and between 10 and 14 km/h. All data are expressed as*
 217 *mean ± SD. ^a significant main foot strike effect. ^b significant running speed effect. ^c significant interaction effect.*

		speed	Forefoot strike	Rearfoot strike
Foot strike angle (°) ^a		10 km/h	-0.4 ± 4.4	14.8 ± 3.7
		14 km/h	0.3 ± 5.3	17.2 ± 5.4
Ratio (%) <i>(E_{TS}/E_{WB})</i>	U03 ^c	10 km/h	26 ± 4	22 ± 8
		14 km/h	25 ± 3	25 ± 8
	B04 ^b	10 km/h	26 ± 3	27 ± 6
		14 km/h	23 ± 4	26 ± 6
	U10 ^b	10 km/h	27 ± 4	28 ± 9
		14 km/h	28 ± 5	32 ± 10
	U16 ^c	10 km/h	27 ± 4	23 ± 8
		14 km/h	26 ± 3	26 ± 9

218

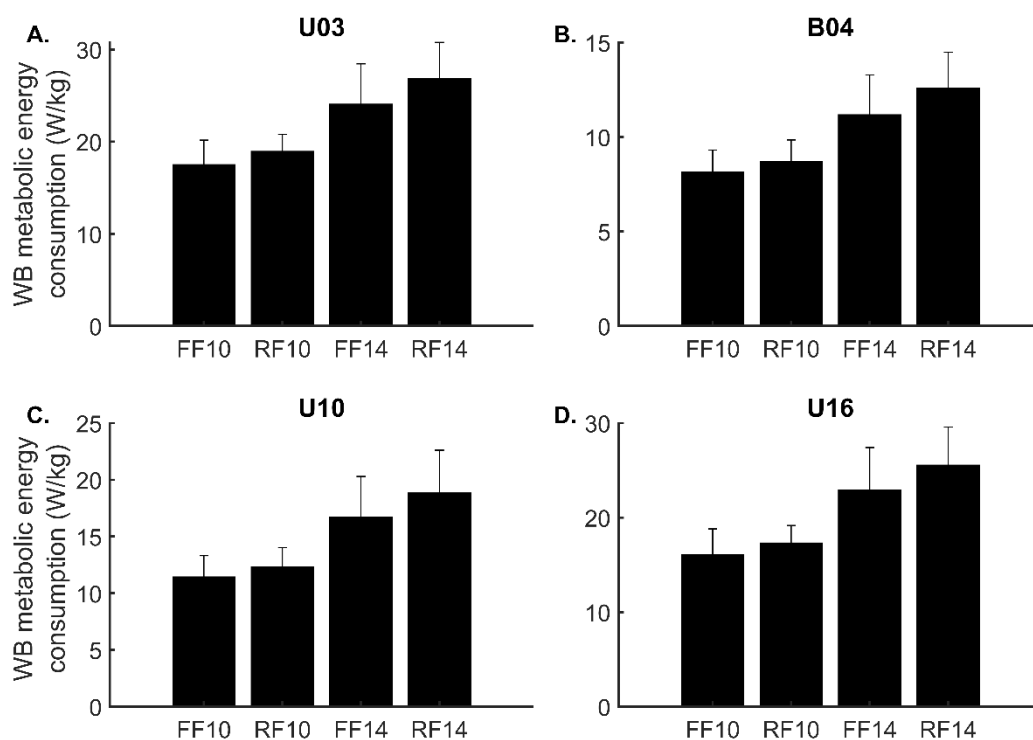


219 *Figure 2. Triceps Surae (TS) metabolic energy consumption including individual muscles: Soleus (black), Gastrocnemius*
 220 *medialis (dark grey) and Gastrocnemius lateralis (light grey) in mid-/forefoot strikers (FF, n = 10) and rearfoot strikers (RF,*
 221 *n = 9). Mixed ANOVA or Mann-Whitney U test demonstrated no significant difference in metabolic energy consumed between*
 222 *foot strike patterns, not for individual Triceps Surae muscle (p > 0.10) nor for all three muscles together (p > 0.35). Mixed*
 223 *ANOVA, paired t-test or Wilcoxon signed-rank test demonstrated significant greater energy consumption at 14km/h compared*
 224 *to 10km/h (p < 0.01).*
 225

226

227 **Discussion**

228 This study investigated the effect of habitual foot strike pattern on simulated Triceps Surae muscle and
229 whole body metabolic energy consumption. We used a dynamic optimization approach in which the
230 Achilles tendon stiffness of the musculoskeletal model was adapted to better match experimental GM
231 ultrasound data (Figure 1). Four different metabolic energy models were incorporated to ensure model
232 independency. In line with our hypothesis, none of the individual Triceps Surae muscles, nor whole
233 body metabolic energy consumption demonstrated significant differences between mid-/forefoot
234 strikers and rearfoot strikers (Figure 2 and Figure 3). Faster running increased both simulated Triceps
235 Surae muscle and whole body metabolic energy consumption.



236

237 **Figure 3. Estimated whole body (WB) metabolic energy consumption for all four metabolic energy models used for mid-**
238 **/forefoot strikers at 10 km/h (FF10) and 14 km/h (FF14) and rearfoot strikers at 10 km/h (RF10) and 14 km/h (RF14).** U03
239 = Umberger, Gerritsen and Martin (2003), B04 = Bhargava, Pandey and Anderson (2004), U10= Umberger (2010) and U16 =
240 Uchida et al. (2016). Mixed ANOVA or Mann-Whitney U test demonstrated no significant difference between foot strike
241 patterns ($p > 0.14$). Mixed ANOVA, paired t-test or Wilcoxon signed-rank test demonstrated significant increase in energy
242 consumption when running at 14 km/h compared to 10 km/h.

243

244 Our results provide additional scientific evidence that mid-/forefoot and rearfoot strike patterns are
245 energetically equivalent. We recently showed that GM muscle force production is greater while muscle
246 contraction velocity is smaller in mid-/forefoot strikers compared to rearfoot strikers, especially during
247 early ground contact (Swinnen et al., 2019). Here, we provide further evidence that the greater muscle
248 forces in mid-/forefoot strikers are more economically produced due to the lower muscle contraction

249 velocities and hence no difference in GM, GL or SOL metabolic energy consumption between foot
250 strike patterns exist. Moreover, previous experimental research already demonstrated that
251 differences in whole body metabolic energy consumption between foot strike patterns are small
252 (Ogueta-Alday et al., 2014) or even non-existing (Cunningham et al., 2010; Gruber et al., 2013; Lussiana
253 et al., 2017; Perl et al., 2012). Studies investigating the effect of gait retraining from rearfoot to
254 forefoot strike running do not find an effect on the metabolic energy consumption during running
255 when enough training sessions (≥ 8) were offered (Ekizos et al., 2018; Roper et al., 2017). However,
256 when only two training sessions were provided an initial increase in metabolic cost is reported (Ekizos
257 et al., 2018), indicating the need for habituation. Hence, since habituation is necessary when switching
258 foot strike pattern and switching ultimately does not result in a reduced metabolic cost, switching foot
259 strike pattern seems to be ineffective from a performance point of view.

260 Next to estimated Triceps Surae muscle and whole body metabolic energy rate, the contribution of the
261 Triceps Surae to the whole body metabolic energy rate (i.e. ratio) was also not different between foot
262 strike patterns. However, the effect of running speed was less clear. Two models (U03 and U16) did
263 not find a speed effect, while U10 and B04 did find a speed effect, but in opposing directions. With
264 faster running the relative contribution of joint power/work during ground contact seems to gradually
265 shift more towards proximal joints (i.e. hip), especially at running speeds closer to sprinting (Schache
266 et al., 2015). Hence, if a shift in muscle metabolic energy consumption would occur, a shift in the same
267 direction as joint power would have been expected, implying a decreased relative contribution of the
268 Triceps Surae with increasing running speed. However, the difference in running speeds tested in this
269 study was small and our fastest speed did not approach sprinting. Therefore, to better understand the
270 effect of running speed on the distribution of muscle metabolic energy consumption across lower
271 extremity muscles a wider range of running speeds should be investigated.

272 Dynamic optimization allowed us to account for muscle-tendon interactions when estimating muscle
273 states. A good match between experimental and predicted muscle states is crucial for good
274 estimations of muscle metabolic energy. We found that it was important to adapt Achilles tendon
275 stiffness to obtain a close match between simulated and measured GM fiber lengths. Using a generic
276 normalized tendon stiffness value of 35 resulted in negligible length changes of the tendinous tissues
277 and as a consequence muscle fascicle length changes were no longer uncoupled from length changes
278 of the entire muscle tendon unit (Fig. S2). Nevertheless, there is ample experimental evidence that the
279 tendinous tissue interacts with the Triceps Surae muscles, uncoupling the muscle fascicle length
280 changes from the length changes of the entire MTU (Fukunaga et al., 2002; Lai et al., 2015; Lichtwark
281 and Wilson, 2008), allowing the muscle fascicles to contract at much slower - more force-efficient -
282 velocities implying lower metabolic energy consumption (Hill, 1922; van der Zee, Lemaire and van

283 Soest, 2019). As a result, predicted Triceps Surae muscle metabolic energy consumption with the
284 generic stiff tendon was on average 80% higher compared to the adapted Achilles tendon stiffness
285 (Fig. S3). Also, estimated whole body metabolic energy consumption was on average 23% higher
286 compared to the adapted Achilles tendon stiffness (Fig. S4). The discrepancy between the results based
287 on the generic and adapted tendon stiffness values illustrates the importance of a good match
288 between computed and experimental muscle states to obtain reliable results of muscle metabolic
289 energy consumption. Moreover, the increased metabolic energy consumption associated with the stiff
290 tendon emphasizes the importance of the muscle-tendon unit interaction on the metabolic energy
291 consumption during running.

292 Although our conclusions are independent of the metabolic energy model used, the wide variability in
293 absolute energy rates between the metabolic energy models are remarkable. While B04 and U10
294 predict experimental whole body metabolic energy consumption rather close to experimental data,
295 whole body metabolic energy consumption predicted by U03 and U16 are almost twice as high as
296 experimentally observed (Batliner et al., 2018; Kipp et al., 2018). The major difference is that U03/U16
297 neglect eccentric work whereas B04/U10 account for eccentric work. Instead of accounting for
298 negative work, U03/U16 reduce the lengthening heat rate coefficient. Our results (lower energy rates
299 with U03/U16) illustrate that the reduction of the lengthening heat rate more than offsets the
300 exclusion of eccentric muscle work. While we seem to have a good understanding of the energy cost
301 of isometric and concentric muscle contractions, the energy cost during eccentric or stretch-shortening
302 muscle contraction is more debatable. It is clear that eccentric muscle work is more efficiently
303 produced compared to concentric muscle work (Hill, 1960), and therefore it appears reasonable to
304 allow eccentric muscle work and muscle lengthening to reduce the metabolic energy consumption rate
305 of a muscle, however a clear consensus on how to treat eccentric work is still lacking. Also the energy
306 cost associated with the stretch-shortening of a muscle is still controversial (Holt et al., 2014; van der
307 Zee et al., 2019). Nevertheless, in contrast to the absolute differences, the relative increase in
308 metabolic energy consumption based on all muscle metabolic models when running faster
309 corresponds quite well with the experimental data. Experimental data indicates that increasing the
310 running speed from 10 km/h to 14 km/h would correspond with an increase in whole body metabolic
311 energy consumption of approximately 40 to 45% (Batliner et al., 2018; Kipp et al., 2018). The energy
312 models predict similar increases of 40% (U03), 41% (B04), 49% (U10) and 45% (U16). In summary, while
313 metabolic energy models do a good job for predicting relative changes, absolute values are not in
314 accordance with experimental data. Therefore, experimental muscle research on how to account for
315 the energy cost of eccentric and stretch-shortening muscle contractions is necessary before
316 recommendations on how to implement these contractions in metabolic energy models can be made.

317 Our study has some limitations. First, we did not measure Achilles tendon stiffness from our
318 participants and assumed equal normalized Achilles tendon stiffness for all subjects. Kubo *et al.* (2015)
319 found no difference in Achilles tendon stiffness between foot strike patterns and thus, on average, we
320 can assume equal normalized Achilles tendon stiffness. Mid-/forefoot strikers are reported to earlier
321 activate their Gastrocnemii muscles (Ahn *et al.*, 2014; Swinnen *et al.*, 2019). However due to our
322 optimization criteria (i.e. minimization of muscle activation squared) pre-activation of the Triceps
323 Surae muscles is not predicted. Still, our simulations demonstrate a slightly earlier Triceps Surae
324 muscle activation in mid-/forefoot strikers than rearfoot strikers (Fig. S1). Furthermore, our
325 musculoskeletal model has some limitations. For example, the musculoskeletal model lacks a midfoot
326 arch, which has been shown to store and release energy and subsequently reduce the metabolic rate
327 during running (Ker *et al.*, 1987; Stearne *et al.*, 2016). Moreover, we only took metabolic energy
328 expenditure during ground contact into account, according to Arellano and Kram (2014) only
329 considering ground contact would lead to an underestimation of 7% of the net metabolic energy
330 expenditure. We used ultrasound data to validate our simulations, a well-known limitation of
331 ultrasound data is that these 2D images represents a 3D muscle structure, possibly resulting in
332 underestimation of muscle fascicle length changes when there is out of plane muscle movement.

333 In conclusion, we demonstrated that – in contrast with the widespread belief in the running
334 community – none of the foot strike patterns induce a reduction in metabolic energy consumption of
335 the Triceps Surae muscle while running. In agreement with previous experimental research, simulated
336 whole body metabolic energy consumption was also similar between foot strike patterns. Hence, we
337 conclude that none of the foot strike patterns can be associated with a superior running energetics.
338 Yet, we looked into differences in metabolic rate during sub-maximal running, an important
339 performance parameter in distance running. It should be noted that for sprinting energy rate is not as
340 important due to the short distance/time.

341 **Acknowledgements**

342

343 **Competing interests**

344 No competing interests declared.

345 **Funding**

346 WS is funded by a PhD fellowship from the research foundation Flanders (11E3919N).

347

348 **References**

- 349 **Ahn, A. N., Brayton, C., Bhatia, T. and Martin, P.** (2014). Muscle activity and kinematics of forefoot
350 and rearfoot strike runners. *J. Sport Heal. Sci.* **3**, 102–112.
- 351 **Altman, A. R. and Davis, I. S.** (2012). A kinematic method for footstrike pattern detection in barefoot
352 and shod runners. *Gait Posture* **35**, 298–300.
- 353 **Arellano, C. J. and Kram, R.** (2014). Partitioning the metabolic cost of human running: A task-by-task
354 approach. *Integr. Comp. Biol.* **54**, 1084–1098.
- 355 **Batliner, M. E., Kipp, S., Grabowski, A. M., Kram, R., Byrnes, W. C., Physiology, I. and States, U.**
356 (2018). Does Metabolic Rate Increase Linearly with Running Speed in all Distance Runners?
357 *Sport. Med. Int. Open* **2**, E1–E8.
- 358 **Bhargava, L. J., Pandy, M. G. and Anderson, F. C.** (2004). A phenomenological model for estimating
359 metabolic energy consumption in muscle contraction. *J. Biomech.* **37**, 81–88.
- 360 **Cavanagh, P. R. and LaFortune, M. A.** (1980). Ground reaction forces in distance running. *J. Biomech.*
361 **13**, 397–406.
- 362 **Cunningham, C. B., Schilling, N., Anders, C. and Carrier, D. R.** (2010). The influence of foot posture
363 on the cost of transport in humans. *J. Exp. Biol.* **213**, 790–797.
- 364 **de Almeida, M. O., Saragiotto, B. T., Yamato, T. P. and Lopes, A. D.** (2015). Is the rearfoot pattern
365 the most frequently foot strike pattern among recreational shod distance runners? *Phys. Ther.*
366 *Sport* **16**, 29–33.
- 367 **De Groote, F., De Laet, T., Jonkers, I. and De Schutter, J.** (2008). Kalman smoothing improves the
368 estimation of joint kinematics and kinetics in marker-based human gait analysis. *J. Biomech.* **41**,
369 3390–3398.
- 370 **De Groote, F., Pipeleers, G., Jonkers, I., Demeulenaere, B., Patten, C., Swevers, J. and De Schutter,**
371 **J.** (2009). A physiology based inverse dynamic analysis of human gait: Potential and
372 perspectives. *Comput. Methods Biomech. Biomed. Engin.* **12**, 563–574.
- 373 **De Groote, F., Kinney, A. L., Rao, A. V. and Fregly, B. J.** (2016). Evaluation of Direct Collocation
374 Optimal Control Problem Formulations for Solving the Muscle Redundancy Problem. *Ann.*
375 *Biomed. Eng.* **44**, 2922–2936.
- 376 **Di Michele, R. and Merni, F.** (2014). The concurrent effects of strike pattern and ground-contact time
377 on running economy. *J. Sci. Med. Sport* **17**, 414–418.
- 378 **Ekizos, A., Santuz, A. and Arampatzis, A.** (2018). Short- and long-term effects of altered point of
379 ground reaction force application on human running energetics. *J. Exp. Biol.* **221**,.
- 380 **Farris, D. J. and Lichtwark, G. A.** (2016). UltraTrack: Software for semi-automated tracking of muscle
381 fascicles in sequences of B-mode ultrasound images. *Comput. Methods Programs Biomed.* **128**,
382 111–118.
- 383 **Fletcher, J. R. and MacIntosh, B. R.** (2017). Running economy from a muscle energetics perspective.
384 *Front. Physiol.* **8**,.
- 385 **Fukunaga, T., Kawakami, Y., Kubo, K. and Kanehisa, H.** (2002). Muscle and Tendon Interaction
386 During Human Movements. *Exerc. Sport Sci. Rev.* **30**, 106–110.
- 387 **Gerus, P., Rao, G. and Berton, E.** (2015). Ultrasound-based subject-specific parameters improve

- 388 fascicle behaviour estimation in Hill-type muscle model. *Comput. Methods Biomech. Biomed.*
389 *Engin.* **18**, 116–123.
- 390 **Gruber, A. H., Umberger, B. R., Braun, B. and Hamill, J.** (2013). Economy and rate of carbohydrate
391 oxidation during running with rearfoot and forefoot strike patterns. *J. Appl. Physiol.* **115**, 194–
392 201.
- 393 **Hamner, S. R., Seth, A. and Delp, S. L.** (2010). Muscle contributions to propulsion and support during
394 running. *J. Biomech.* **43**, 2709–2716.
- 395 **Handsfield, G. G., Meyer, C. H., Hart, J. M., Abel, M. F. and Blemker, S. S.** (2014). Relationships of 35
396 lower limb muscles to height and body mass quantified using MRI. *J. Biomech.* **47**, 631–638.
- 397 **Hasegawa, H., Yamauchi, T. and Kraemer, W. J.** (2007). Foot strike patterns of runners at the 15-km
398 point during an elite-level half marathon. *J. Strength Cond. Res.* **21**, 888–893.
- 399 **Hill, A. V** (1922). The maximum work and mechanical efficiency of human muscles, and their most
400 economical speed. *J. Physiol.* **56**, 19–41.
- 401 **Hill, A. V.** (1960). Production and absorption of work by muscle. *Science* **131**, 897–903.
- 402 **Holt, N. C., Roberts, T. J. and Askew, G. N.** (2014). The energetic benefits of tendon springs in
403 running: is the reduction of muscle work important? *J. Exp. Biol.* **217**, 4365–4371.
- 404 **Hoogkamer, W., Kipp, S., Spiering, B. A. and Kram, R.** (2016). Altered running economy directly
405 translates to altered distance-running performance. *Med. Sci. Sports Exerc.* **48**, 2175–2180.
- 406 **Jones, A. M. and Carter, H.** (2000). The effect of endurance training on parameters of aerobic fitness.
407 *Sport. Med.* **29**, 373–386.
- 408 **Kasmer, M. E., Liu, X. C., Roberts, K. G. and Valadao, J. M.** (2013). Foot-strike pattern and
409 performance in a marathon. *Int. J. Sports Physiol. Perform.* **8**, 286–292.
- 410 **Ker, R. F., Bennett, M. B., Bibby, S. R., Kester, R. C. and Alexander, R. M.** (1987). The spring in the
411 arch of the human foot. *Nature* **325**, 147–149.
- 412 **Kipp, S., Grabowski, A. M. and Kram, R.** (2018). What determines the metabolic cost of human
413 running across a wide range of velocities? *J. Exp. Biol.* **221**, jeb184218.
- 414 **Kipp, S., Kram, R. and Hoogkamer, W.** (2019). Extrapolating metabolic savings in running:
415 Implications for performance predictions. *Front. Physiol.* **10**,.
- 416 **Kram, R. and Taylor, R. C.** (1990). Energetics of running: a new perspective. *Nature* **346**, 265–267.
- 417 **Kubo, K., Miyazaki, D., Tanaka, S., Shimoju, S. and Tsunoda, N.** (2015). Relationship between
418 Achilles tendon properties and foot strike patterns in long-distance runners. *J. Sports Sci.* **33**,
419 665–669.
- 420 **Lai, A., Lichtwark, G. A., Schache, A. G., Lin, Y.-C., Brown, N. A. T. and Pandy, M. G.** (2015). In vivo
421 behavior of the human soleus muscle with increasing walking and running speeds. *J. Appl.*
422 *Physiol.* **118**, 1266–1275.
- 423 **Larson, P., Higgins, E., Kaminski, J., Decker, T., Preble, J., Lyons, D., McIntyre, K. and Normile, A.**
424 (2011). Foot strike patterns of recreational and sub-elite runners in a long-distance road race. *J.*
425 *Sports Sci.* **29**, 1665–1673.
- 426 **Lichtwark, G. A. and Wilson, A. M.** (2008). Optimal muscle fascicle length and tendon stiffness for
427 maximising gastrocnemius efficiency during human walking and running. *J. Theor. Biol.* **252**,
428 662–673.

- 429 **Lussiana, T., Gindre, C., Hébert-Losier, K., Sagawa, Y., Gimenez, P. and Mourot, L.** (2017). Similar
430 running economy with different running patterns along the aerial-terrestrial continuum. *Int. J.*
431 *Sports Physiol. Perform.* **12**, 481–489.
- 432 **Mercer, J. A. and Horsch, S.** (2015). Heel-toe running: A new look at the influence of foot strike
433 pattern on impact force. *J. Exerc. Sci. Fit.* **13**, 29–34.
- 434 **Miller, R. H.** (2014). A comparison of muscle energy models for simulating human walking in three
435 dimensions. *J. Biomech.* **47**, 1373–1381.
- 436 **Ogueta-Alday, A., Rodríguez-Marroyo, J. A. and García-López, J.** (2014). Rearfoot striking runners
437 are more economical than midfoot strikers. *Med. Sci. Sports Exerc.* **46**, 580–585.
- 438 **Patterson, M. A. and Rao, A. V.** (2014). GPOPS-II. *ACM Trans. Math. Softw.* **41**, 1–37.
- 439 **Perl, D. P., Daoud, A. I. and Lieberman, D. E.** (2012). Effects of footwear and strike type on running
440 economy. *Med. Sci. Sports Exerc.* **44**, 1335–1343.
- 441 **Roper, J. L., Doerfler, D., Kravitz, L., Dufek, J. S. and Mermier, C.** (2017). Gait Retraining from
442 Rearfoot Strike to Forefoot Strike does not change Running Economy. *Int. J. Sports Med.* **38**,
443 1076–1082.
- 444 **Schache, A. G., Brown, N. A. T. and Pandy, M. G.** (2015). Modulation of work and power by the
445 human lower-limb joints with increasing steady-state locomotion speed. *J. Exp. Biol.* **218**, 2472–
446 2481.
- 447 **Stearne, S. M., Alderson, J. A., Green, B. A., Donnelly, C. J. and Rubenson, J.** (2014). Joint kinetics in
448 rearfoot versus forefoot running: Implications of switching technique. *Med. Sci. Sports Exerc.*
449 **46**, 1578–1587.
- 450 **Stearne, S. M., McDonald, K. A., Alderson, J. A., North, I., Oxnard, C. E. and Rubenson, J.** (2016). The
451 Foot's Arch and the Energetics of Human Locomotion. *Sci. Rep.* **6**,.
- 452 **Swinnen, W., Hoogkamer, W., Delabastita, T., Aeles, J., De Groote, F. and Vanwanseele, B.** (2019).
453 Effect of habitual foot-strike pattern on the gastrocnemius medialis muscle-tendon interaction
454 and muscle force production during running. *J. Appl. Physiol.* **126**, 708–716.
- 455 **Uchida, T. K., Hicks, J. L., Dembia, C. L. and Delp, S. L.** (2016). Stretching your energetic budget: How
456 tendon compliance affects the metabolic cost of running. *PLoS One* **11**, 1–19.
- 457 **Umberger, B. R.** (2010). Stance and swing phase costs in human walking. *J. R. Soc. Interface* **7**, 1329–
458 40.
- 459 **Umberger, B. R., Gerritsen, K. G. M. and Martin, P. E.** (2003). A Model of Human Muscle Energy
460 Expenditure. *Comput. Methods Biomech. Biomed. Engin.* **6**, 99–111.
- 461 **van der Zee, T. J., Lemaire, K. K. and van Soest, A. J.** (2019). The metabolic cost of in vivo constant
462 muscle force production at zero net mechanical work. *J. Exp. Biol.* **222**, jeb199158.
- 463 **Wächter, A. and Biegler, L. T.** (2006). On the implementation of an interior-point filter line-search
464 algorithm for large-scale nonlinear programming. *Math. Program.* **106**, 25–57.
- 465 **Waters, R. L. and Mulroy, S.** (1999). The energy expenditure of normal and pathologic gait. *Gait*
466 *Posture* **9**, 207–231.
- 467 **Zajac, F. E.** (1989). Muscle and tendon: properties, models, scaling, and application to biomechanics
468 and motor control. *Crit. Rev. Biomed. Eng.* **17**, 359–410.
- 469